

Chemical and Isotopic Fractionation of Lead in the surface soils of Egypt

Waleed H. Shetaya^{1,*}, Ezzat R. Marzouk², Elham F. Mohamed¹, Elizabeth H. Bailey³,
Scott D. Young³

¹Air Pollution Research Department, Environmental Research Division, National Research Centre, 33 El-Bohouth St., Dokki, Giza 12622, Egypt

²Division of Soil and Water Sciences, Faculty of Environmental Agricultural Sciences, Arish University, North Sinai, 45516, Egypt

³Division of Agricultural and Environmental Sciences, School of Biosciences, University of Nottingham, Sutton Bonington, Leicestershire LE12 5RD, UK

*Corresponding Author: Waleed H. Shetaya, +201012632019, wh.shetaya@nrc.sci.eg; waleed.shetaya@outlook.com

39 **Abstract**

40 Chemical fractionation via sequential extraction (SEP) combined with isotopic analysis of Pb was used
41 to investigate the origins and reactivity of Pb in 66 topsoil samples collected from 12 different locations
42 in Egypt. The total soil Pb concentrations (TPb) covered a wide range (~ 80 – 16,000 mg kg⁻¹), but
43 were only elevated in four industrial and urban locations within Cairo and Alexandria. In all the other
44 locations values of TPb were generally low and were close to the average crustal Pb concentration of
45 14 mg kg⁻¹. The largest Pb fraction in all soils, with the exception of two industrial locations, was the
46 'residual' fraction (38 – 63% of TPb) followed by Pb bound to 'organic' and 'metal oxide' phases. The
47 Pb isotopic signatures (²⁰⁶Pb/²⁰⁷Pb vs ²⁰⁸Pb/²⁰⁷Pb) of all samples in all SEP fractions were highly
48 variable, suggesting a heterogeneous mix of Pb contamination sources; however, they aligned closely
49 to a binary mixing line between geogenic and petrol Pb sources. There were similar patterns across all
50 of the non-residual fractions with measureable data (F2 – F4) suggesting that the non-residual
51 anthropogenic-Pb and geogenic-Pb have been assimilated into common pools within the soil. Binary
52 and ternary source-apportionment models based on Pb isotopic ratios and abundances showed that
53 the relative contribution of petrol-Pb and geogenic-Pb can be ascribed with reasonable certainty.
54 However, the contribution of further sources can only be accounted for if the isotopic abundance of all
55 end-members are known and are at the periphery of the soils dataset.

56

57 **Keywords:**

58 Environmental Pollution; Heavy Metals; Sequential Extraction; Stable Isotopes; ICP-MS

59

60

61

62

63

64

65

66

67

68

69 **1. Introduction**

70 Lead (Pb) is listed by the WHO as a chemical of major public health concern because of its high toxicity
71 to living organisms (WHO, 2010). Long-term exposure of humans and animals to low levels of Pb
72 through inhalation and/or ingestion may lead to a range of adverse clinical complications including
73 neurological, cardiovascular and renal damage (Needleman and Bellinger, 1991). Geogenic Pb is
74 composed of four stable isotopes: ^{208}Pb (52%), ^{206}Pb (24%), ^{207}Pb (23%) and ^{204}Pb (1%); the only
75 primordial isotope is ^{204}Pb , while the others are the fission products of uranium and thorium (Komárek
76 et al., 2008). Therefore, the isotopic composition of Pb varies between different geological sources and
77 this can be used as a tool to identify sources of pollutant Pb and to study its environmental fate
78 (Veysseyre et al., 2001).

79

80 The large scale industrialization and urbanization of Egypt since the 1950's, in addition to the common
81 practice of open air incineration of agriculture and other waste (Mohamed et al., 2015), were associated
82 with the emission of large amounts of pollutants (including Pb) to the atmosphere. As a result, by the
83 late 1980's and early 1990's Pb in the atmosphere of urban Egypt reached deleterious concentrations
84 (Hassanien and Horvath, 1999, Nasralla and Ali, 1984, Shakour and El-Taieb, 1994). However, due to
85 the introduction of the Environment Law in 1994 and the implementation of several environmental
86 protection measures, such as relocating lead smelters and phasing out leaded petrol, the concentration
87 of atmospheric Pb in urban Egypt reached safe levels by the end of the 1990's (Hassan et al., 2013,
88 Hassanien et al., 2001, Rizk and Khoder, 2001, Safar and Labib, 2010). Nevertheless, most of the
89 legacy anthropogenic-Pb which has been deposited on surface soils may not have been fully
90 assimilated into the same soil fractions as geogenic-Pb. The bioavailability and mobility of contaminant
91 Pb is therefore difficult to predict and it may be transferred to food and fodder crops and surface or
92 ground waters more readily than geogenic-Pb.

93

94 Measuring total concentrations of heavy metals in soils may not always be a useful approach for risk
95 assessment because, frequently, only a small proportion of soil metal is mobile under natural conditions
96 (Tack and Verloo, 1995, Teutsch et al., 2001). It is therefore useful to estimate the labile, and potentially
97 bioavailable, metal pool alongside the total concentration (Meers et al., 2007, Young et al., 2000).
98 Sequential extraction protocols (SEP) have been used to investigate the chemical fractionation and

99 potential availability of heavy metals in soils. Possibly the most established SEP is the one developed
100 by Tessier et al. (1979) which provides a guide to the likely chemical form of metals in soil or the
101 adsorption phases with which the metals are associated. In the Tessier SEP, five operational fractions
102 are identified: (F1) Exchangeable (metal fractions desorbed due to changes in the ionic composition of
103 soil solution), (F2) Bound to carbonates (metal fractions reactive to pH fluctuations), (F3) Bound to Fe
104 and Mn oxides (fractions that can be released by reduction of oxides under low Eh conditions), (F4)
105 Bound to organic matter (metal fractions released under strong oxidizing conditions), and (F5) Residual
106 (metal fractions held within the crystal structure of soil minerals).

107

108 The main aim of this work was to assess the current reactivity of Pb, and identify its origins, in Egyptian
109 soils two decades after phasing out leaded petrol and implementing countermeasures to Pb pollution.
110 This was achieved by studying the chemical fractionation and isotopic composition of Pb in some
111 Egyptian surface soils and the soil properties likely to control them. A total of 66 soil samples that had
112 been exposed to different degrees of Pb contamination were collected and characterized. Soil metals
113 were chemically fractionated based on the SEP procedure of Tessier et al. (1979). The isotopic
114 abundances of the four stable Pb isotopes were also measured in the SEP extracts by inductively
115 coupled plasma mass spectrometry (ICP-MS). The objective was to assess the degree of assimilation
116 of anthropogenic-Pb (mainly petrol-Pb) and geogenic Pb, into each soil Pb fraction (Shetaya et al.,
117 2018). Moreover, multiple-sources models were used to try to identify the relative contribution of petrol,
118 geogenic and industrial Pb sources, to different soil phases, based on their Pb isotopic signatures.

119

120

121

122

123

124

125

126

127

128

129 2. Materials and Methods

130 2.1. Soil sampling

131 Sixty six topsoil samples (0 – 20 cm) were collected, along a transect 0 - 100 m away from main roads,
132 from 12 different locations in Egypt representing industrial, urban, agriculture and background sites
133 (Table 1). Industrial locations included a cement factory (HE-I), inactive lead smelter (SH-I) and a major
134 waste water treatment facility (CA-I). Urban soils were sampled around major motorways within the
135 largest two urban conurbations in Egypt: Greater Cairo (CA-U and SH-U) and Alexandria (AX-U), in
136 addition to Ismailia City (IS-U) and Assiut-Minya desert motorway (AM-U). Agriculture soils were
137 collected from arable fields within Ismailia (IS-G) and Sharkia (SK-G) governorates. Reference
138 (background) soils were sampled from 2 rural locations that were expected to have been exposed to
139 minimal Pb deposition or discharge including sites in the Sinai Peninsula (SI-B) and Suez governorate
140 (SZ-B). Soils were collected with a clean stainless steel trowel and sealed in plastic bags for transport.

141 **Table 1.** Sampling locations, codes and description. Letters I, U, G and B at the end of sample codes
142 refer to the industrial, urban, agriculture and background nature of the sampling location, respectively.

Site nature	Location	Code	Number of Soil Samples	Coordinates
Industrial	Cairo - Helwan	HE-I (Cement Factory)	4	29.83N, 31.31E
	Cairo - Shubra	SH-I (Lead Smelter)	4	30.11N, 31.27E
	Cairo - Khanka	CA-I (Waste Water Treatment)	4	30.20N, 31.37E
Urban and Motorways	Cairo - Ring Road	CA-U	10	30.17N, 31.35E
	Alexandria	AX-U	5	31.15N, 29.97E
	Cairo - Shubra	SH-U	8	30.14N, 31.25E
	Ismailia	IS-U	8	30.59N, 32.27E
	Assiut - Minya	AM-U	4	27.93N, 30.57E
Agriculture	Ismailia	IS-G	4	30.68N, 32.05E
	Sharkia	SK-G	4	30.64N, 31.70E
Background	Sinai	SI-B	3	30.83N, 34.14E
	Suez	SZ-B	8	30.10N, 32.57E

143

144 2.2. Characterization of soil samples

145 Soil samples were air dried at room temperature and then sieved to <2 mm particle size; a fraction of
146 each sample was finely ground with an agate ball mill (Retsch PM400). To measure soil pH, 5 g of the
147 sieved soils, were suspended in 12.5 mL MQ water (18.2 MΩ cm) and shaken end-over-end for 30 min;
148 pH was measured with a glass electrode allowing 5 min for equilibration. The organic carbon content
149 of the soils was determined with a CN analyzer (Elementar VarioMax) after carbonates were removed
150 with 50% HCl. Available phosphorus was extracted with 0.5 M sodium bicarbonate (NaHCO₃) solution

151 at pH 8.5 (Olsen et al., 1954) and assayed using a variation on the phosphomolybdate method
152 (Drummond and Maher, 1995) by measuring absorbance in a 1 cm cell at 880 nm (CE 1011
153 spectrophotometer, Cecil Instruments). Amorphous (reactive) Fe, Al and Mn oxides were extracted from
154 the finely ground soils by the citrate-bicarbonate-dithionite protocol developed by Kostka and Luther
155 (1994); total Fe, Al and Mn concentrations in the filtered supernatants were assayed by ICP-MS. Total
156 soil Pb (TPb) and total phosphorus (P) content were assayed by ICP-MS following digestion of 0.2 g
157 finely ground soil samples in an acid mixture composed of Primar Plus™ or Analytical grade HF (2.5
158 mL; 40%), HNO₃ (2 mL; 70%), HClO₄ (1 mL; 70%) and H₂O (2.5 mL).

159 **2.3. Sequential Extraction of Pb**

160 All soil samples were extracted, in duplicate, by a sequential extraction procedure (SEP) adapted from
161 that of Li and Thornton (2001) which was originally developed by Tessier et al. (1979) as shown below.

- 162 1- Exchangeable fraction (F1): 1 g soil samples (<2mm sieved) were extracted in polycarbonate
163 centrifuge tubes for 20 min with 8 mL 0.5 M MgCl₂.
- 164 2- Bound to carbonate fraction (F2): the residues from F1 were extracted with 8 mL 1 M CH₃COONa
165 (adjusted to pH 5 with CH₃COOH) for 5 hours.
- 166 3- Bound to iron and manganese oxides (F3): the residues from F2 were extracted with 10 mL 0.04
167 M hydroxylamine hydrochloride in 25% (v/v) CH₃COONa at 96°C in a water bath for 6 h with
168 occasional agitation.
- 169 4- Bound to organic matter (F4): the residues from F3 were extracted with 3 mL 0.02 M HNO₃ and 5
170 mL 30% H₂O₂ (adjusted to pH 2 with HNO₃) and tubes were heated to 85°C in a water bath and
171 maintained for 2 h with occasional agitation. Three mL H₂O₂ (adjusted to pH 2 with HNO₃) were
172 then added and tubes were heated again for 3 h at 85°C with intermittent agitation. After cooling,
173 5 mL 3.2 M CH₃COONa in 20% (v/v) HNO₃ were added and the tubes were agitated for 30 min.

174 Sample tubes were centrifuged after each extraction step and the supernatant solutions were syringe
175 filtered and retained for multi-element and Pb isotopic analysis by ICP-MS; the remaining soil was
176 retained for the next extraction step. Carry-over from the previous step was accounted for
177 gravimetrically.

178 The concentration of Pb (mg kg⁻¹) in the residual phase (F5) was calculated by subtracting the
179 summation of Pb concentrations (mg kg⁻¹) in the first four steps (F1-F4) from total soil Pb (TPb)

180 measured in the HF-HClO₄-HNO₃ acid soil digestates. For quality assurance, the recovery of the SEP
181 procedure was tested on 11 samples in which the residual fraction was digested in a mixture of HF-
182 HClO₄-HNO₃ for 19 h (Atkinson et al., 2011); 95 – 110 % recovery was achieved for Pb.

183 The individual isotopic concentrations of Pb in the residual fraction (F5) were obtained from the isotopic
184 abundances (IA) of the total soil Pb and fractions F1 to F4. (Eq. 1).

$$185 \quad {}^X\text{Pb}_{F5} = \text{TPb} \cdot {}^X\text{IA}_T - (\text{Pb}_{F1} \cdot {}^X\text{IA}_{F1} + \text{Pb}_{F2} \cdot {}^X\text{IA}_{F2} + \text{Pb}_{F3} \cdot {}^X\text{IA}_{F3} + \text{Pb}_{F4} \cdot {}^X\text{IA}_{F4}) \quad (1)$$

186 where, ${}^X\text{Pb}_{F5}$ is the concentration (mol kg⁻¹) of a ${}^X\text{Pb}$ isotope (²⁰⁴Pb, ²⁰⁶Pb, ²⁰⁷Pb or ²⁰⁸Pb) in the residual
187 fraction (F5); TPb and Pb_{F1, F2, F3 or F4} are the total soil and non-residual fraction (F1, F2, F3 or F4)
188 concentrations of Pb (mol kg⁻¹), respectively; ${}^X\text{IA}_T$ and ${}^X\text{IA}_{F1, F2, F3 \text{ or } F4}$ are the total soil and non-residual
189 (F1, F2, F3 or F4) isotopic abundances of ${}^X\text{Pb}$.

190 No attempts were made to investigate artificial isotopic fractionation of Pb during the sequential
191 extraction procedure. However, heavy atoms e.g. Pb isotopes with very small fractional differences in
192 atomic mass would not support mass-dependent fractionation during chemical processes on any
193 significant level (Bacon et al., 2006, Komárek et al., 2008, Lee and Yu, 2016, Monna et al., 1997). This
194 was also found to be true for even much lighter elements e.g. Fe and Cu with relatively large fractional
195 differences in atomic mass (Roebbert et al., 2018).

196 **2.4. Elemental and isotopic analyses by ICP-MS**

197 Concentrations of Pb, P, Fe, Al and Mn in soil digestates and extracts were determined using ICP-MS
198 (Model iCAPQ; Thermo Fisher Scientific GmbH, Bremen, Germany) as described in Shetaya et al.
199 (2018). Briefly, samples and multi-element calibration standards (Certiprep/Fisher, UK) were diluted in
200 2% Primar Plus™ grade HNO₃ and measured in triplicate. Internal standards, including Rh and Ir in
201 2% HNO₃ were introduced to the sample stream via a t-piece. Limits of detection (LOD) were calculated
202 from analysis of 16 blanks. Montana soil reference material (NIST 2711) was used for quality assurance
203 and 96 ± 4% average recovery was achieved across all measured elements.

204 The ²⁰⁴Pb, ²⁰⁶Pb, ²⁰⁷Pb and ²⁰⁸Pb isotopic abundances in all samples were measured with a short dwell
205 time of 2.5 ms and a total of 10,000 sweeps were used to mitigate the effects of 'plasma flicker' and
206 achieve a high level of precision. For *internal* mass bias correction, a Tl solution (10 µg L⁻¹), was
207 introduced directly to the internal standard line and the variations in the ²⁰³Tl/²⁰⁵Tl ratios were used to

208 correct shifts in Pb isotopic ratios (Blum and Bergquist, 2007, Shetaya et al., 2017). In addition, drift in
209 mass bias was corrected *externally* by repeatedly assaying the certified Pb isotope standard NIST-981
210 and using linear interpolation to correct CPS ratios to isotopic ratios for samples (Atkinson et al., 2011,
211 Marzouk et al., 2013b). To reduce polyatomic interferences from $^{92}\text{Os}-^{16}\text{O}$ (208 mass), $^{193}\text{Ir}-^{14}\text{N}$ (207
212 mass) and $^{205}\text{Tl}-\text{H}$ (206 mass), the ICP-MS was used in the kinetic energy discrimination (KED) mode
213 with helium as a collision gas. The isobaric interference to ^{204}Pb from ^{204}Hg was corrected by
214 determining intensity at $m/z = 202$ (^{202}Hg) and, from expected isotopic ratios, subtracting the intensity
215 (CPS) attributed to ^{204}Hg within the instrument software. However, in practice the overall contribution of
216 ^{204}Hg to the intensity at m/z 204 was trivial and the average ratio of $^{204}\text{Hg}/^{204}\text{Pb}$ in the measured soil
217 fractions was estimated as 0.0033. All solutions were diluted to ensure that the detector operated in
218 'pulse-counting' mode; data were rejected and sample analysis repeated, after appropriate dilution, if
219 the detector 'tripped' to an analogue measurement in response to large count rates, typically > 1.5
220 million counts s^{-1} for the ^{208}Pb isotope (Marzouk et al., 2013a).

221 **2.5. Binary and ternary source apportionment**

222 Frequently, two identifiable sources of Pb are apparently present in soil, arising from (i) the petrol
223 additive tetra-methyl Pb ('Petrol-Pb') and (ii) the underlying parent material ('Geogenic-Pb'). As a first
224 approximation, we can then add a (single) third source, which is considered to originate from a range
225 of industrial and power generation sources ('Industrial'). This may be similar to the Geogenic-Pb if there
226 is a local source of coal or Pb ore.

227 The proportional contribution (%) of any two Pb sources (e.g. Petrol, Geogenic or Industrial), to total
228 soil Pb (TPb) or total Pb concentration in any of the SEP fractions, was calculated from Eq. 2 (Lee and
229 Yu, 2016, Mao et al., 2014).

$$230 \quad \% \text{Pb}_A = \frac{\text{IR}_T - \text{IR}_B}{\text{IR}_A - \text{IR}_B} \times 100 \quad (2)$$

231 where, $\% \text{Pb}_A$ is the proportion of TPb from source A; IR_A and IR_B are the Pb isotopic ratios ($^{206}\text{Pb}/^{207}\text{Pb}$
232 or $^{208}\text{Pb}/^{207}\text{Pb}$) of sources A and B, respectively; IR_T is the measured Pb isotopic ratio ($^{206}\text{Pb}/^{207}\text{Pb}$ or
233 $^{208}\text{Pb}/^{207}\text{Pb}$) of the whole soil or any individual SEP fraction (F1 – F5).

234 The relative contribution of three different end-member (pure) sources was modeled using Eq. 3 and
235 Eq. 4 adapted from Cheng and Hu (2010) and Luo et al. (2015).

236 $\%Pb_A + \%Pb_B + \%Pb_C = 100\%$ (3)

237 where, $\%Pb_A$, $\%Pb_B$ and $\%Pb_C$ are the proportions of Pb from sources A, B and C to TPb or total Pb in
238 any of the five SEP fractions.

239 ${}^xIA_T = \%Pb_A {}^xIA_A + \%Pb_B {}^xIA_B + \%Pb_C {}^xIA_C$ (4)

240 where, xIA_T is the isotopic abundance of a xPb isotope (${}^{204}Pb$, ${}^{206}Pb$, ${}^{207}Pb$ or ${}^{208}Pb$) in soil or individual
241 SEP fractions; xIA_A , xIA_B and xIA_C are the isotopic abundances of the same isotope in the pure sources
242 A, B and C.

243 The 'Solver' function in the software package Excel 2017 was used to minimize the residual standard
244 deviation (RSD) between the modelled and measured isotopic abundances of all soils simultaneously.
245 The operation was performed independently for total soil Pb (TPb) and for Pb in all of the five SEP
246 fractions (F1 – F5).

247 The anthropogenic-Pb isotopic distribution, in any soil phase (total or F1 – F5), was calculated by
248 subtracting geogenic-Pb from total Pb (TPb) assuming uniform distribution of geogenic-Pb across the
249 studied terrains (Eq. 5).

250 ${}^xPb_{AT} = Pb_T {}^xIA_T - Pb_G {}^xIA_G$ (5)

251 where, ${}^xPb_{AT}$ is the anthropogenic concentration (mol kg⁻¹) of an isotope (${}^{204}Pb$, ${}^{206}Pb$, ${}^{207}Pb$ or ${}^{208}Pb$), in
252 any soil phase (total or F1 – F5); Pb_T and Pb_G are the total soil Pb and geogenic-Pb concentrations (mol
253 kg⁻¹), respectively (in the respective soil fraction); xIA_T and xIA_G are the isotopic abundances in total and
254 geogenic Pb, respectively.

255 These approaches only present a simplified image of a complex geochemical system where soil Pb is
256 a mixture of numerous sources. However, potentially they provide a means of quantifying the relative
257 contribution of the two or three major Pb sources to each soil SEP fraction.

258

259

260

261 **3. Results and Discussion**

262 **3.1. Soil Properties**

263 Key soil parameters are shown in Table 2. Total soil Pb concentrations (TPb) in the studied locations
264 are discussed in detail by Shetaya et al. (2018). Briefly, TPb was greatest at the lead smelter site (SH-
265 I), peaking at ~ 31,000 mg kg⁻¹ with an average of ~ 16,200 mg kg⁻¹. This was followed by the industrial
266 location CA-I (waste water treatment) and the urban locations CA-U and AX-U within Cairo and
267 Alexandria with average TPb values of 171, 160, and 82.6 mg kg⁻¹, respectively. However, significant
268 difference ($p < 0.05$; 2 sample t-test; Minitab 17) were only found between CA-I and AX-U locations. All
269 other non-background locations showed relatively low TPb levels with an average of 17 mg kg⁻¹ which
270 is slightly above the Pb average crustal abundance of 14 mg kg⁻¹ (Emsley, 2011) indicating generally
271 low levels of Pb contamination in the soils of Egypt. All soils, with the exception of a few individual
272 samples, were alkaline and organic-poor (pH 8 and 1% SOC on average) likely due to the calcareous
273 and sandy marine origins of Egyptian soils (Shaheen, 2009).

274

275

276

277

278

279

280

281

282 **Table 2.** Soil parameters including total soil Pb (TPb), soil pH, organic content (%SOC), available P (Olsen) and total P, and reactive Al, Mn and Fe
 283 oxides; n = number of samples in each location and NA = not available (not measured). Letters I, U, G and B at the end of sample codes refer to
 284 the industrial, urban, agriculture and background nature of the sampling location, respectively.

Location	n	Total Pb (TPb) ($mg\ kg^{-1}$)				pH		SOC (%)		Available P ($mg\ kg^{-1}$)		Total P ($g\ kg^{-1}$)		Al ₂ O ₃ ($g\ kg^{-1}$)		MnO ₂ ($g\ kg^{-1}$)		Fe ₂ O ₃ ($g\ kg^{-1}$)	
		Mean	SD	Max.	Min.	Mean	SD	Mean	SD	Mean	SD	Mean	SD	Mean	SD	Mean	SD	Mean	SD
Industrial																			
HE-I	4	19.5	2.83	23.5	16.9	9.7	1.3	0.95	0.19	27.9	7.47	0.24	0.06	1.08	0.77	0.02	0	3.21	1.01
SH-I	4	16201	15788	30808	2494	8	0.2	2.31	2.52	85.3	20.5	1.06	1.17	2.8	2.47	0.08	0.01	5.62	1.98
CA-I	4	171	14.2	184	157	8.3	0	3.48	0.61	215	23.1	0.14	0.11	2.5	1.35	0.23	0.33	4.6	5.68
Urban																			
CA-U	10	160	185	459	8.04	8.2	0.2	0.90	0.35	13.4	12.3	0.63	0.24	2.29	0.81	0.6	0.32	7.61	3.32
AX-U	5	82.6	94.6	247	18.3	7.8	0.7	3.20	1.92	NA	NA	0.4	0.05	30.5	8.68	0.59	0.12	30.3	9.84
SH-U	8	25.4	10.3	37.6	11.9	7.8	0.2	0.96	0.79	39.6	43.1	1.13	0.46	2.53	0.18	0.6	0.08	13.1	4.92
IS-U	8	18.7	11.1	40.5	6.47	7.9	0.2	0.52	0.50	13.2	10.7	0.28	0.15	1.31	0.32	0.09	0.05	2.67	0.79
AM-U	4	10.3	2.56	12	5.81	8.5	0.5	0.11	0.06	1.8	0.34	0.33	0.05	1.15	0.5	0.01	0.02	2.26	0.62
All data	35	68.5	119	459	5.81	8	0.4	1.33	1.49	18.6	25.5	0.57	0.39	9.09	13.3	0.44	0.3	12.9	12.1
Agriculture																			
IS-G	4	6.66	0.26	6.97	6.35	8.5	0.2	0.15	0.07	5.14	6.83	0.27	0.17	0.73	0.17	0.03	0.01	1.09	0.72
SK-G	4	11	0.73	11.6	10.2	7.8	0	0.29	0.04	9.24	5.95	0.59	0.04	2.03	0.03	0.21	0	3.51	0.05
All data	8	8.78	2.31	11.6	6.35	8.1	0.4	0.22	0.09	7.19	5.74	0.43	0.21	1.38	0.76	0.12	0.11	2.30	1.46
Background																			
SI-B	3	9.87	4.63	15.1	6.34	7.9	0.2	2.21	3.36	NA	NA	0.52	0.34	17.1	4.65	0.24	0.13	10.4	5.36
SZ-B	8	3.37	1.60	5.84	1.90	7.8	0.1	0.05	0.04	NA	NA	1.19	1.39	1.5	0.43	0.03	0.05	1.31	0.44
All data	11	4.96	3.21	15.1	1.90	8	0.2	1.07	1.53	NA	NA	0.68	0.75	15.5	12.8	0.15	0.11	7.38	5.38

285

286

287

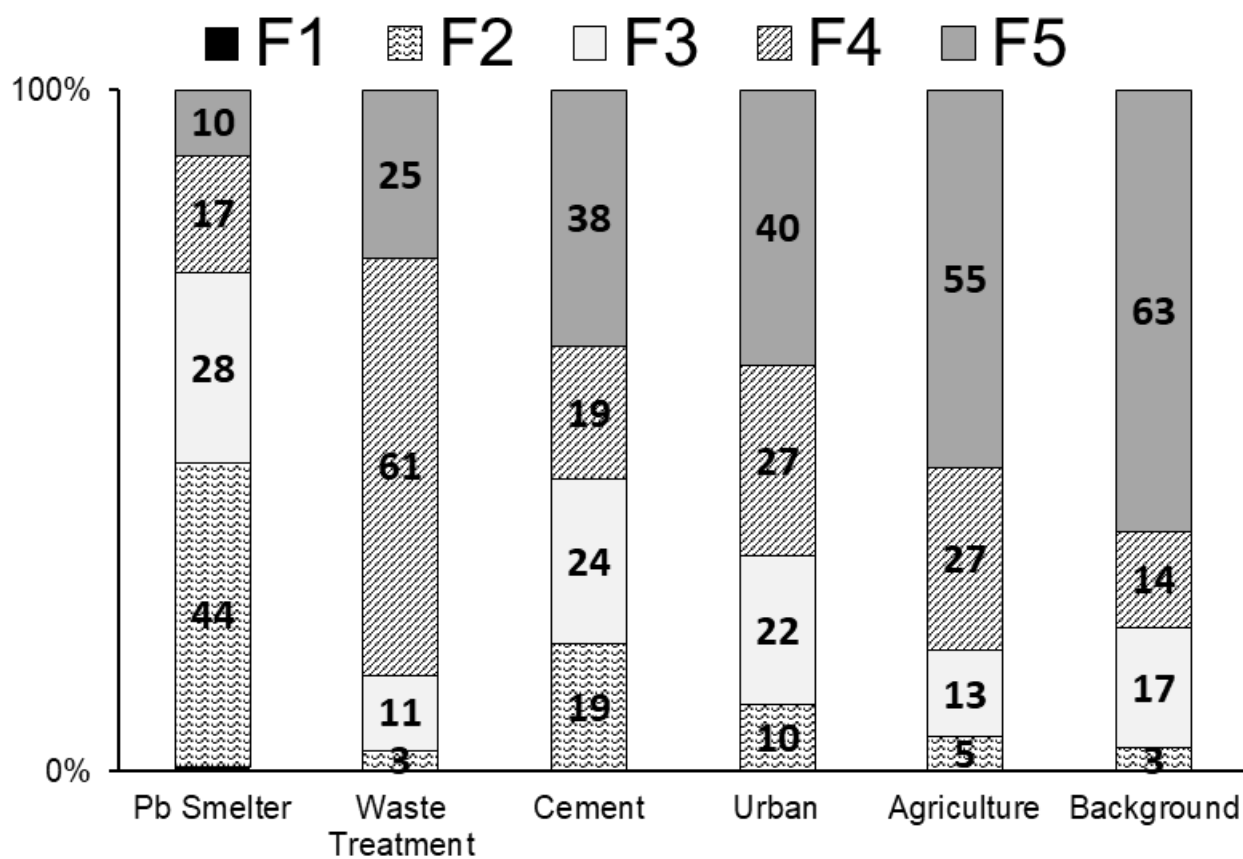
288 **3.2. Geochemical fractions of Pb determined by sequential extraction (SEP)**

289 The proportion (%) of residual (non-reactive) Pb fraction (F5-Pb) was highest in the background sites
290 followed by agriculture, urban and industrial locations, respectively (Figure 1 and Table A.1); on average,
291 F5-Pb was inversely proportional to TPb ($R^2 = 0.97$; power relationship) (Figure A.1). Since the residual
292 fraction (F5) represents Pb in primary and secondary minerals, e.g. galena (PbS) and pyromorphite
293 ($Pb_5(PO_4)_3Cl$), that hold Pb within their crystal structure (Cotter-Howells and Thornton, 1991, Tessier et al.,
294 1979), the exchange of F5-Pb with other soil phases is likely to be extremely slow and limited. This means
295 that any anthropogenic inputs of Pb will be almost exclusively distributed among the non-residual phases
296 (F1-F4) and that F5-Pb is mostly geogenic in origin. As the anthropogenic input of Pb increased (higher
297 TPb), Pb in F5-Pb proportionally decreased resulting in the inverse relationship between TPb and F5-Pb.
298 This is also supported by the fact that F5-Pb was the largest fraction in the background, agriculture, urban
299 and cement factory locations (relatively low TPb) as opposed to the lead smelter (SH-I) and waste water
300 treatment (CA-I) sites (highest TPb) where the percentages of F5-Pb were only 10% and 25% of TPb, on
301 average, respectively.

302 The second and third largest fractions in all soils, with the exception of SH-I and CA-I, were, respectively,
303 F3 (bound to metal oxides) and F4 (bound to organic). In alkaline soils, these two phases are likely to be
304 the most important non-residual phases for retention of heavy metals (Atkinson et al., 2011, Li and
305 Thornton, 2001, Tipping et al., 1986)

306 Location CA-I (waste water treatment) was dominated by F4-Pb (61%) possibly due to its markedly elevated
307 organic content (3.5% SOC) in comparison to all other locations ($P < 0.005$; paired t-test) (Table 1). The
308 largest fraction (44%) in location SH-I (lead smelter) was F2 (bound to carbonates). Li and Thornton (2001)
309 also reported high F2-Pb levels (24 – 55%) in mining and smelting sites with substantially elevated TPb
310 concentrations. Although, in mining locations, the high concentration of F2-Pb was attributed to the sheer
311 abundance of the thermodynamically favored cerussite ($PbCO_3$) (Brookins, 2012), the large F2-Pb fraction
312 in smelting sites may be due to the ability of CH_3COONa to dissolve PbO (Clevenger et al., 1991) which is
313 a primary emission product of lead smelters (Foster and Lott, 1980). Moreover, Murphy (1992) found that
314 $PbCO_3$ is one of the major weathering products in the soils around old smelting facilities.

315 The exchangeable fraction (F1) was only detectable in locations SH-I (1%) and CA-U (0.3%) (Figure 1 and
 316 Table A.1). In alkaline soils Pb ions are strongly adsorbed and exchangeable Pb (F1-Pb) is likely to be a
 317 very minor fraction (McBride, 1994, Sparks, 2003). However, when Pb levels are largely elevated, such as
 318 is location SH-I (lead smelter), Pb ions will occupy progressively weaker sorption sites and so the proportion
 319 of exchangeable Pb increases (Degryse et al., 2009, Sastre et al., 2006, Tongtavee et al., 2005). In
 320 addition, PbSO₄, which is an important component of Pb smelter emissions (Clevenger et al., 1991, Foster
 321 and Lott, 1980), may be initially incorporated into the exchangeable phase (F1) (Harrison et al., 1981).



322
 323 **Figure 1.** Proportion (%) of Pb estimated in each of the five SEP fractions: F1 (exchangeable), F2 (bound
 324 to carbonates), F3 (bound to metal oxides), F4 (bound to organic matter) and F5 (residual). Industrial
 325 locations (Pb smelter, waste water treatment, and cement factory) are displayed independently due to their
 326 different nature, agriculture and background sites are grouped together by site type. Numbers inside the
 327 boxes represent the proportion (%) of each fraction to total soil Pb (TPb). Detailed data is displayed in Table
 328 A.1.

329

330 **3.3. Isotopic fractionation of Pb in soil phases**

331 The isotopic ratios (IR) $^{206}\text{Pb}/^{207}\text{Pb}$ and $^{208}\text{Pb}/^{207}\text{Pb}$ measured or calculated in all SEP fractions (F1 – F5)
332 are shown in Table 3 for all sampling locations. Note that F1-Pb was below detection limit in most samples
333 and the calculation of F5-Pb IR (Eq. 1) produced reliable results only in soils where F5-Pb concentrations
334 were $\geq 40\%$ of TPb (c. $> 50\%$ of the samples) due to compounded errors in Eq. 1 where F5 was a minor
335 constituent of TPb. Shetaya et al. (2018) reported that petrol-Pb (IR of 1.11 ± 0.002 for $^{206}\text{Pb}/^{207}\text{Pb}$ and
336 2.385 ± 0.002 for $^{208}\text{Pb}/^{207}\text{Pb}$) and geogenic-Pb (IR values of 1.212 ± 0.004 for $^{206}\text{Pb}/^{207}\text{Pb}$ and $2.482 \pm$
337 0.006 for $^{208}\text{Pb}/^{207}\text{Pb}$) are likely to be the two major sources of Pb in the soils of Egypt. Figure 2 clearly
338 shows that the IRs $^{206}\text{Pb}/^{207}\text{Pb}$ and $^{208}\text{Pb}/^{207}\text{Pb}$ for all soils in all five SEP fractions are aligned closely to a
339 binary mixing line between the isotopic signatures of the two end members (nominally 'petrol' and
340 'geogenic'). This suggests that these are the two major contributors to both non-residual and residual Pb
341 fractions in the studied soils with only minor contributions from other potential sources contributing to
342 scattering of the data around the binary line. This agrees with the findings of other studies that adopted the
343 binary plot approach to resolve the likely major sources of Pb using the isotopic signatures of two 'pure'
344 end members. For example, Monna et al. (1997) found that the Pb isotopic signatures of various
345 environmental samples from UK and France were aligned around a mixing line between geogenic-Pb
346 ($^{206}\text{Pb}/^{207}\text{Pb} \approx 1.17 - 1.19$) and petrol-Pb ($^{206}\text{Pb}/^{207}\text{Pb} \approx 1.05 - 1.08$). Chenery et al. (2012), Izquierdo et al.
347 (2012) and Mao et al. (2014) also found that the Pb isotopic signatures of their investigated UK samples
348 (soils, plants and aerosols) indicated an almost exclusive mixing between petrol-Pb ($^{206}\text{Pb}/^{207}\text{Pb} \approx 1.06 -$
349 1.09) and Pb from indigenously mined coal ($^{206}\text{Pb}/^{207}\text{Pb} \approx 1.16 - 1.21$). This seems to be a universal pattern
350 at least in the European environments where the Pb signatures of environmental samples align around a
351 binary line between geogenic-Pb ($^{206}\text{Pb}/^{207}\text{Pb} \approx 1.22 - 1.24$) and petrol-Pb ($^{206}\text{Pb}/^{207}\text{Pb} \approx 1.12 - 1.14$)
352 (Komárek et al., 2008).

353 To investigate the isotopic distribution of Pb in relation to their SEP phase, the $^{206}\text{Pb}/^{207}\text{Pb}$ IR of all soils
354 were plotted against total soil Pb (TPb) (Figure 3). In all five SEP fractions (F1- F5), Pb isotopic signatures
355 formed discrete clusters according to their origins. Soils from the background location (SZ-B) were grouped
356 very close to the geogenic-Pb isotopic ratio while soils from urban (TPb $< 100 \text{ mg kg}^{-1}$), agriculture and
357 cement factory locations were distributed between geogenic-Pb and petrol-Pb indicating broadly similar

358 contributions from both sources. Waste treatment locations and urban soils with TPb > 100 mg kg⁻¹ were
359 more inclined toward the petrol-Pb isotopic signature. In all soil fractions, locations with higher values of
360 TPb were inclined toward the petrol signature of ²⁰⁶Pb/²⁰⁷Pb.

361 Lead smelter (SH-I) soils also formed clusters with ²⁰⁶Pb/²⁰⁷Pb IRs that fell between those of geogenic-Pb
362 and petrol-Pb in all four non-residual Pb fractions (Figure 3 A – D); however, given the much greater Pb
363 concentrations in these soils, it is likely that the smelter would generate a unique ²⁰⁶Pb/²⁰⁷Pb signature and
364 the contribution of geogenic-Pb and petrol-Pb at this location was probably trivial in comparison. This is
365 supported by the fact that the Pb smelting facility that was located in this site was recycling scrap lead from
366 various industries and sources e.g. old batteries, and most of this recycled Pb was originally imported rather
367 than indigenously mined (Labib et al., 2003, Safar et al., 2014). The measured ²⁰⁶Pb/²⁰⁷Pb ratios (1.151 –
368 1.155) in SH-I site, in all non-residual phases, agreed well with the average ‘industrial’ ²⁰⁶Pb/²⁰⁷Pb ratios
369 (1.147 - 1.160) reported by Monna et al. (1997).

370 Most samples showed almost identical patterns across the non-residual (F2, F3 and F4) phases (Figure 3
371 B – D). Bacon et al. (2006) and Lee and Yu (2016) also reported homogenous distributions of Pb IRs
372 among non-residual soil phases in spite of distinct Pb isotopic signatures between Pb sources, soil depths
373 and sampling locations. In our work, the apparent consistency of Pb isotopic signatures among non-residual
374 phases is also statistically supported (paired t-test; Minitab 17) by insignificant differences between
375 ²⁰⁶Pb/²⁰⁷Pb or ²⁰⁸Pb/²⁰⁷Pb ratios of the non-residual fractions, with the single exception of ²⁰⁶Pb/²⁰⁷Pb when
376 comparing F3 and F4 (Table A.2). Comparison with F1-Pb and F5-Pb isotopic signatures could not be
377 discussed with confidence due to the limited number of valid results; however, the few available data points
378 (Figure 3 A and E) appear to resemble those of F2, F3 and F4 (Figure 3 B - D).

379 The similarity of isotopic signatures across the fractions (F1 - F5) may indicate that Pb from anthropogenic
380 sources (petrol and other) may have no preferential affinity for specific non-residual or residual soil phases
381 and has been sufficiently labile to be assimilated into common pools with geogenic-Pb due to prolonged
382 contact with the soil. However, isotopic homogeneity between fractions should be interpreted carefully
383 because differences in the Pb isotopic abundances between SEP fractions may only be measurable if a
384 given Pb source, with a distinct isotopic signature, had a high chemical affinity for specific soil phases

385 resulting in limited mixing between fractions. This would depend on both the Pb source speciation and the
386 soil chemical properties. Our collection of soils fell within a relatively narrow range of properties (Table 2)
387 thus potentially contributing to the apparent Pb isotopic homogeneity between the non-residual (and
388 possibly residual) fractions. Furthermore, sequential extraction procedures are prone to re-adsorption
389 effects which may have contributed to the similarity in the Pb isotopic patterns between the non-residual
390 fractions. *Mass-dependent* fractionation of Pb between different soil phases is likely to be very small due
391 to the high mass of the Pb isotopes and would not be detectable by a quadrupole ICP.

392

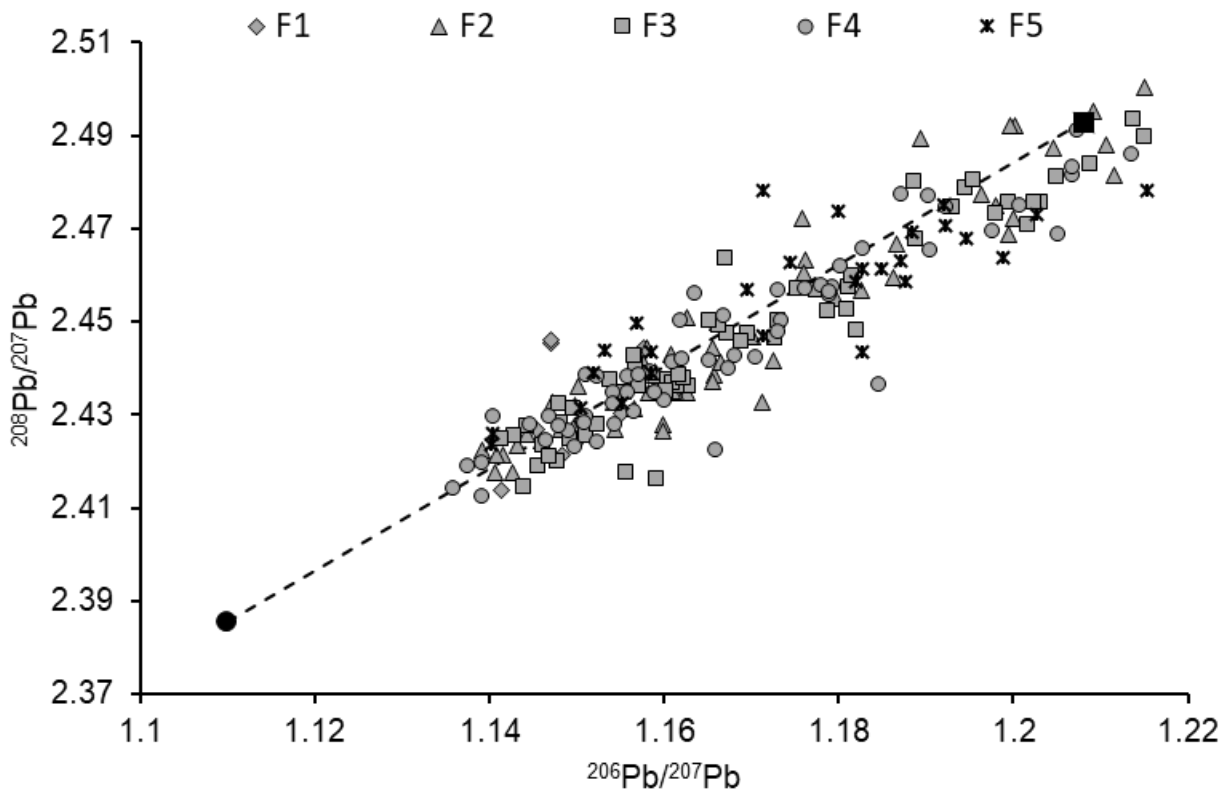
393 **Table 3.** Isotopic ratios ($^{206}\text{Pb}/^{207}\text{Pb}$ and $^{208}\text{Pb}/^{207}\text{Pb}$) measured in the four SEP fractions: F1= exchangeable, F2=bound to carbonates, F3=bound
 394 to Fe/Mn reactive oxides, F4=bound to organic matter, F5=Residual. n = number of samples in each location, SD= standard deviation between soils
 395 sampled from the same site, ND = not detectable (below detection limit), NM= not measured and NA = not applicable.

Sampling Locations	n	F1				F2				F3				F4				F5			
		$^{206}\text{Pb}/^{207}\text{Pb}$		$^{208}\text{Pb}/^{207}\text{Pb}$		$^{206}\text{Pb}/^{207}\text{Pb}$		$^{208}\text{Pb}/^{207}\text{Pb}$		$^{206}\text{Pb}/^{207}\text{Pb}$		$^{208}\text{Pb}/^{207}\text{Pb}$		$^{206}\text{Pb}/^{207}\text{Pb}$		$^{208}\text{Pb}/^{207}\text{Pb}$		$^{206}\text{Pb}/^{207}\text{Pb}$		$^{208}\text{Pb}/^{207}\text{Pb}$	
		Mean	SD	Mean	SD	Mean	SD	Mean	SD	Mean	SD	Mean	SD	Mean	SD	Mean	SD	Mean	SD	Mean	SD
Industrial																					
HE-I	4	ND	NA	ND	NA	1.159	0.011	2.441	0.008	1.161	0.012	2.437	0.013	1.161	0.014	2.437	0.014	1.149	0.013	2.431	0.011
SH-I	4	1.151	0.008	2.425	0.009	1.155	0.016	2.435	0.013	1.152	0.006	2.421	0.007	1.151	0.005	2.433	0.006	NA	NA	NA	NA
CA-I	4	ND	NA	ND	NA	1.141	0.001	2.419	0.002	1.144	0.002	2.425	0.002	1.139	0.001	2.420	0.007	NA	NA	NA	NA
Urban																					
CA-U	10	1.148	0.008	2.424	0.020	1.169	0.023	2.453	0.029	1.167	0.021	2.444	0.022	1.164	0.021	2.443	0.021	1.183	0.017	2.457	0.014
AX-U	5	NM	NA	NM	NA	NM	NA	NM	NA	NM	NA	NM	NA	NM	NA	NM	NA	NM	NA	NM	NA
SH-U	8	ND	NA	ND	NA	1.161	0.004	2.437	0.006	1.166	0.006	2.444	0.008	1.163	0.011	2.443	0.009	1.257	0.143	2.822	0.430
IS-U	8	ND	NA	ND	NA	1.156	0.007	2.433	0.006	1.156	0.006	2.435	0.009	1.158	0.005	2.437	0.010	1.169	0.017	2.460	0.019
AM-U	4	ND	NA	ND	NA	1.199	0.014	2.474	0.013	1.202	0.015	2.483	0.011	1.190	0.019	2.467	0.020	1.165	0.021	2.450	0.017
All data	35	NA	NA	NA	NA	1.167	0.019	2.446	0.022	1.168	0.019	2.447	0.020	1.166	0.018	2.445	0.017	1.186	0.051	2.506	0.173
Agriculture																					
IS-G	4	ND	NA	ND	NA	1.172	0.013	2.448	0.028	1.172	0.010	2.451	0.010	1.172	0.016	2.457	0.021	1.162	0.013	2.445	0.013
SK-G	4	ND	NA	ND	NA	1.174	0.011	2.453	0.009	1.176	0.005	2.455	0.006	1.176	0.004	2.453	0.007	1.181	0.001	2.466	0.011
All data	8	ND	NA	ND	NA	1.173	0.011	2.450	0.020	1.174	0.007	2.453	0.008	1.174	0.011	2.455	0.015	1.168	0.014	2.452	0.016
Background																					
SI-B	3	NM	NA	NM	NA	NM	NA	NM	NA	NM	NA	NM	NA	NM	NA	NM	NA	NM	NA	NM	NA
SZ-B	8	ND	NA	ND	NA	1.203	0.006	2.486	0.011	1.200	0.005	2.477	0.004	1.192	0.019	2.462	0.025	1.196	0.019	2.461	0.012
All data	11	NA	NA	NA	NA	1.203	0.006	2.486	0.011	1.200	0.005	2.477	0.004	1.192	0.019	2.462	0.025	1.196	0.019	2.461	0.012

396

397

398



399

400 **Figure 2.** Isotopic ratios ($^{206}\text{Pb}/^{207}\text{Pb}$ vs $^{208}\text{Pb}/^{207}\text{Pb}$) of the F1, F2, F3, F4 and F5 SEP fractions in all soil
 401 samples. Petrol-Pb (black circle) and geogenic-Pb (black square) signatures are also shown as two
 402 possible end members; the dashed line is the mixing line between them. F5 fraction signatures are shown
 403 for samples where F5-Pb was $\geq 40\%$ of total soil Pb (TPb).

404

405

406

407

408

409

410

411

412

413

414

415

416

417

418

419

420

421

422

423

424

425

426

427

428

429

430

431

432

433

434

435

436

437

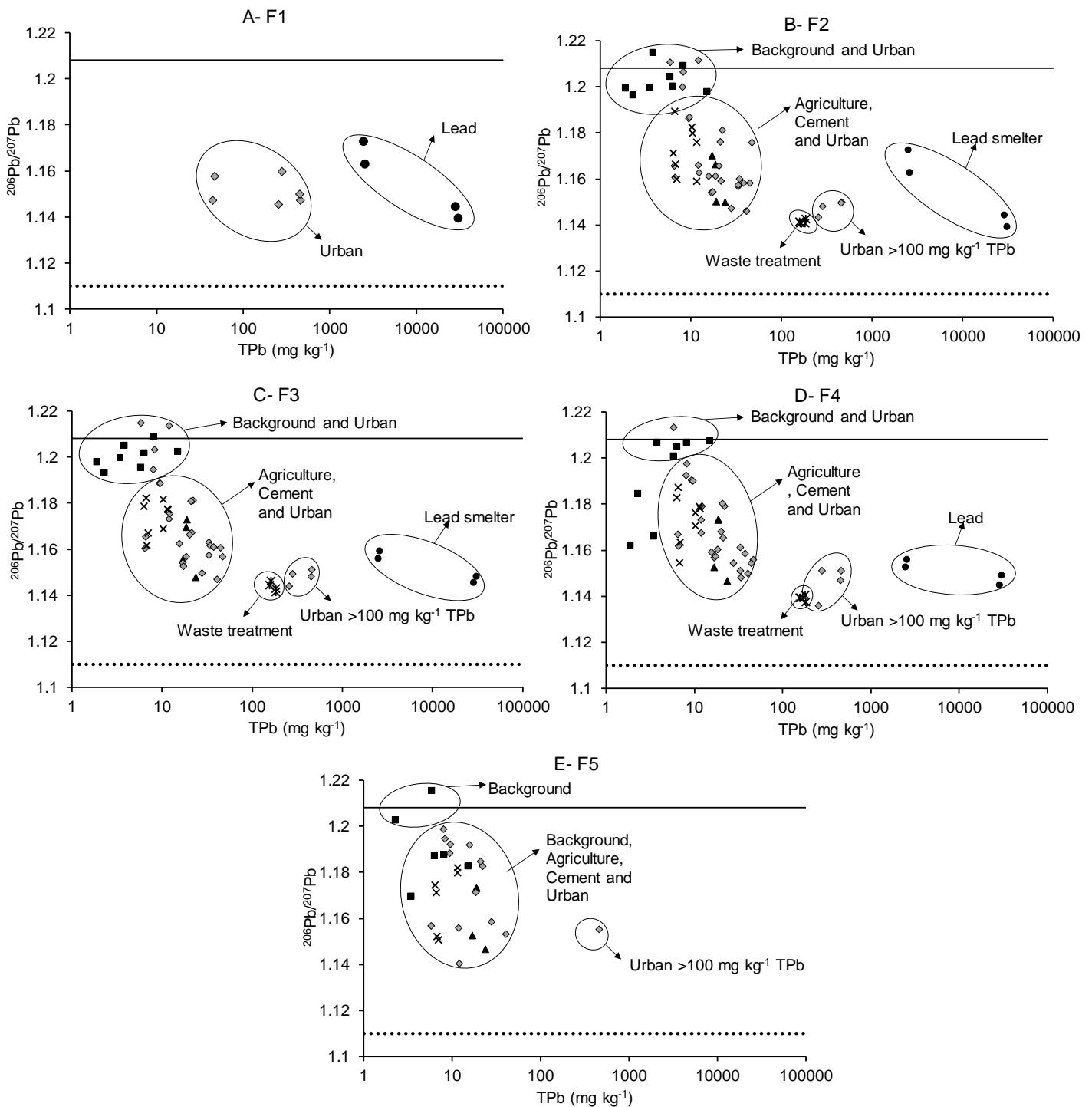


Figure 3. Isotopic ratios ²⁰⁶Pb/²⁰⁷Pb vs total soil Pb (TPb; mg kg⁻¹) for all SEP fractions: F1 (A), F2 (B), F3 (C), F4 (D) and F5 (E). Sampling locations included lead smelter (black circles), waste water treatment (asterisks), urban (grey diamonds), agriculture (crosses), cement factory (black triangles) and background (black squares). Solid and dotted lines represent the ²⁰⁶Pb/²⁰⁷Pb ratios of geogenic-Pb and petrol-Pb, respectively.

438 **3.4. Relative contribution of geogenic and petrol Pb pools**

439 The proportional contributions (%) of petrol-Pb and geogenic-Pb in non-residual fractions F2, F3 and F4 in
440 all soils, except SH-I (lead smelter) soils, were estimated from Eq. 2. Figure 4 shows that the greatest
441 proportion of petrol-Pb was found in the industrial location CA-I (wastewater treatment) with 66, 68 and
442 70% of Pb in fractions F3, F2 and F4, respectively. This was followed by the cement factory (HE-I) and
443 urban locations where there were almost equal proportions of petrol-Pb and geogenic-Pb. Agricultural
444 locations were characterized by low petrol-Pb contributions (34 – 36%) to all fractions while background
445 locations were dominated (84 – 91%) by geogenic-Pb. Overall, higher total soil Pb (TPb) concentrations
446 resulted in a greater proportion of petrol-Pb in all fractions.

447 It appears from Figure 4 that the proportion of Petrol-Pb was consistent within all fractions. As mentioned
448 previously (section 3.3), measurable differences in the distribution of anthropogenic-Pb between soil
449 phases would require a high affinity of the emitted Pb for one particular phase and very slow mixing between
450 fractions. However, the evidence from this study suggests that the different sources of Pb have effectively
451 mixed between (SEP) fractions.

452

453

454

455

456

457

458

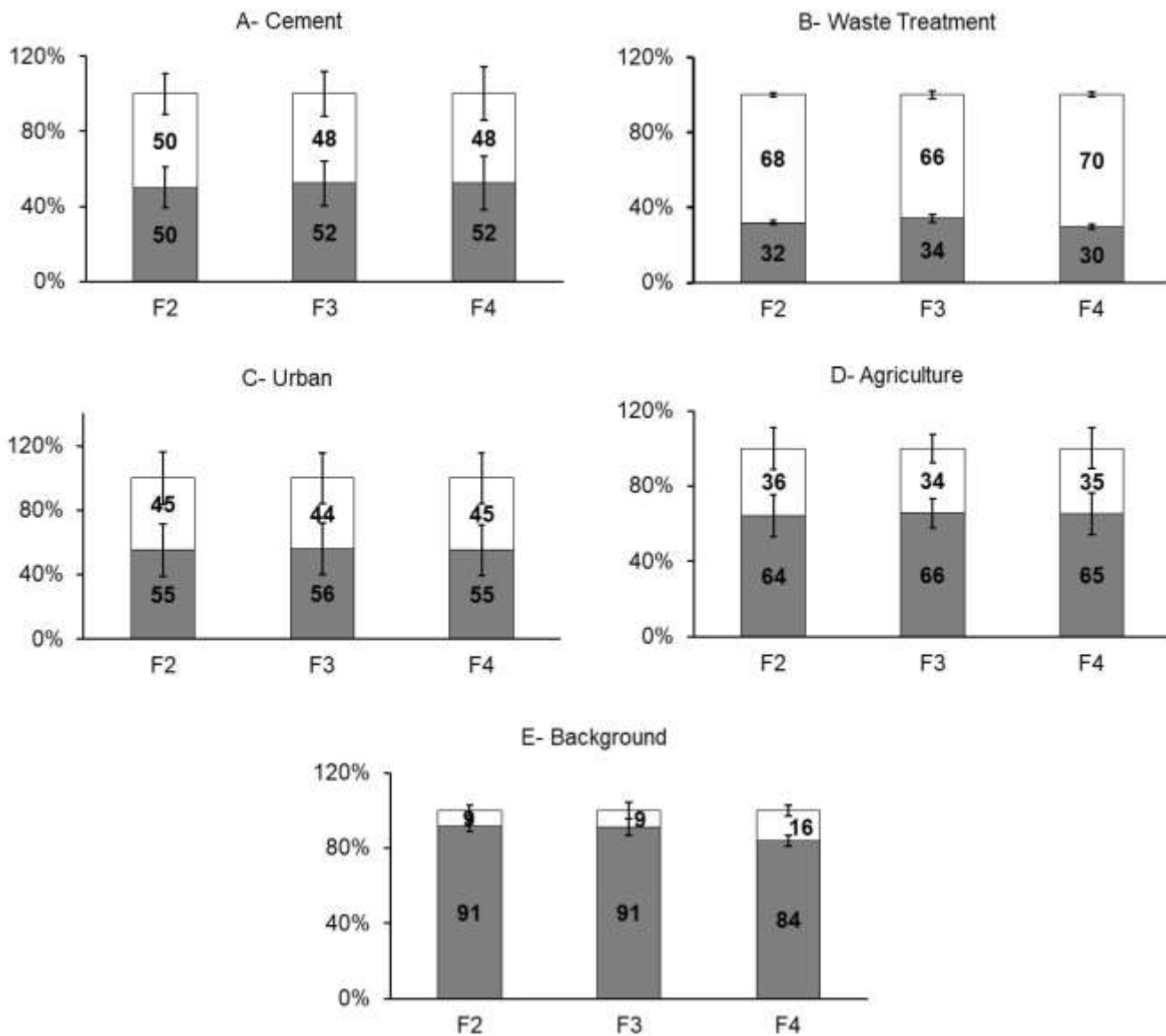
459

460

461

462

463
 464
 465
 466
 467
 468
 469
 470
 471
 472
 473
 474
 475
 476
 477
 478
 479
 480
 481
 482
 483
 484
 485
 486



487
 488
 489
 490
 491
 492
 493
 494

Figure 4. Proportion (%) of petrol-Pb (white boxes) and geogenic-Pb (dark grey boxes) in the non-residual fractions F2, F3 and F4 in all sampling locations, excluding the SH-I (lead smelter) samples. Numbers inside the boxes represent the proportion (%) of each fraction relative to total Pb in the respective soil phase. Error bars represent the standard deviation between soils from the same location.

495 **3.5. Interpreting Pb isotopic signatures assuming three sources**

496 We investigated the possibility of modelling the contribution of a third 'industrial' Pb contribution to the total
497 Pb pool in addition to the geogenic-Pb and petrol-Pb end-members in all soil phases. As discussed
498 previously (section 3.3), soils from the Lead Smelter location (SH-I) are likely to have a distinct isotopic
499 signature (IR of 1.14 for $^{206}\text{Pb}/^{207}\text{Pb}$ and 2.41 for $^{208}\text{Pb}/^{207}\text{Pb}$ for total soil Pb) that is independent in origin
500 from the other two definable sources (petrol-Pb and geogenic-Pb). This smelting facility recycled lead from
501 various industries that used imported Pb metal, so it seemed possible that the Pb signature of the SH-I
502 location soil may represent the range of Pb used industrially in Egypt. As such, the smelter site could be
503 considered as representing a third Pb isotope end-member.

504 However, the IA values of ^{208}Pb in the smelter samples were too low to represent a discrete end member.
505 To resolve a *hypothetical* third Pb source (designated 'industrial Pb'), it was necessary to lower the isotopic
506 abundances (IA) of ^{204}Pb , ^{206}Pb , ^{207}Pb using a factor of 0.985, allowing the ^{208}Pb IA to compensate by
507 keeping the sum of IA values equal to 1. The 'Solver' function of Excel together with Eq. 3 and Eq. 4 (as
508 described in section 2.5) was then employed to find an optimum 'industrial' end-member for TPb and the
509 SEP fractions across all soils simultaneously. The best fit between modelled and measured isotopic
510 abundances of ^{206}Pb , ^{207}Pb and ^{208}Pb was achieved with IR values of 1.14 for $^{206}\text{Pb}/^{207}\text{Pb}$ and 2.48 for
511 $^{208}\text{Pb}/^{207}\text{Pb}$ in the 'industrial' source (Figure A.2). The resulting contributions of all three hypothetical Pb
512 sources (petrol, geogenic and industrial) are shown in Figure 5. The industrial-Pb source contribution was
513 relatively uniform across all soils and soils fractions ranging from 13 – 28% of TPb. The relative contribution
514 of petrol-Pb and geogenic Pb displayed similar patterns to that observed with the binary model (section 3.5;
515 Figure 4) showing considerably higher geogenic-Pb contributions in the background and agriculture soils
516 (Figure 5 D and E), almost equal contribution of both sources in the cement factory location (Figure 5 A)
517 and a larger contribution from petrol-Pb in the waste treatment location.

518 In an alternative approach, the anthropogenic-Pb isotopic abundances were calculated by subtracting an
519 estimate of the geogenic-Pb contribution from total Pb in all soil fractions (Eq. 5). Geogenic Pb isotope
520 concentrations were estimated from the average Pb concentration and isotopic abundances of the
521 background location SZ-B. This approach assumes a uniform distribution of geogenic-Pb in the studied

522 soils arising from similar underlying geological Pb concentrations and isotopic signatures across all the
523 studied terrains. The molar concentrations of all four (anthropogenic) Pb isotopes were then calculated
524 from Eq. 5. Figure 6 shows the isotopic signatures of the calculated anthropogenic-Pb in all soil fractions.
525 However, it was apparent that the 'removal' of such a small background Pb content produced little change
526 in the distribution of Pb isotopes and the 'anthropogenic' isotopic ratios of Pb were distributed between
527 petrol-Pb and geogenic-Pb and well beyond the Pb smelter data (higher $^{206}\text{Pb}/^{207}\text{Pb}$ ratios) provisionally
528 assumed to represent the 'industrial Pb' signature. The smelter Pb is certainly a candidate source for the
529 mix of Pb in Egyptian soils – and this is consistent with the fact that it falls on the periphery of the soil Pb
530 isotope ratio dataset (Figure 6). However, it is also clear from the position of the majority of the soil data in
531 Figure 6 that the Pb smelter cannot serve as a single 'industrial-Pb' source in Egypt and must be regarded
532 as a contributory factor. Figure 6 clearly indicates that a more general pool of (non-petrol) 'industrial-Pb' in
533 Egypt must have a Pb isotope signature closer to that of Egyptian geogenic-Pb.

534

535

536

537

538

539

540

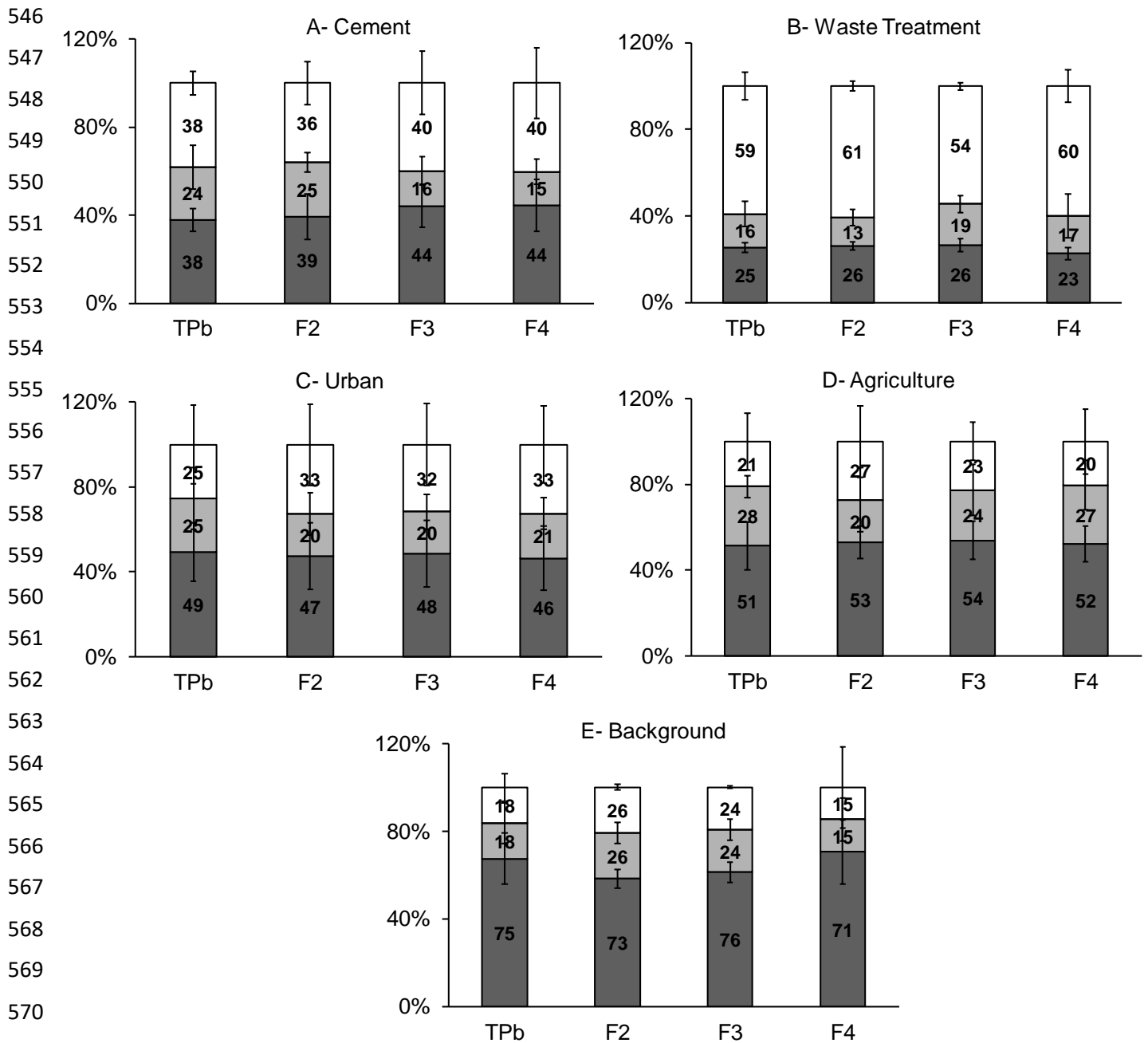
541

542

543

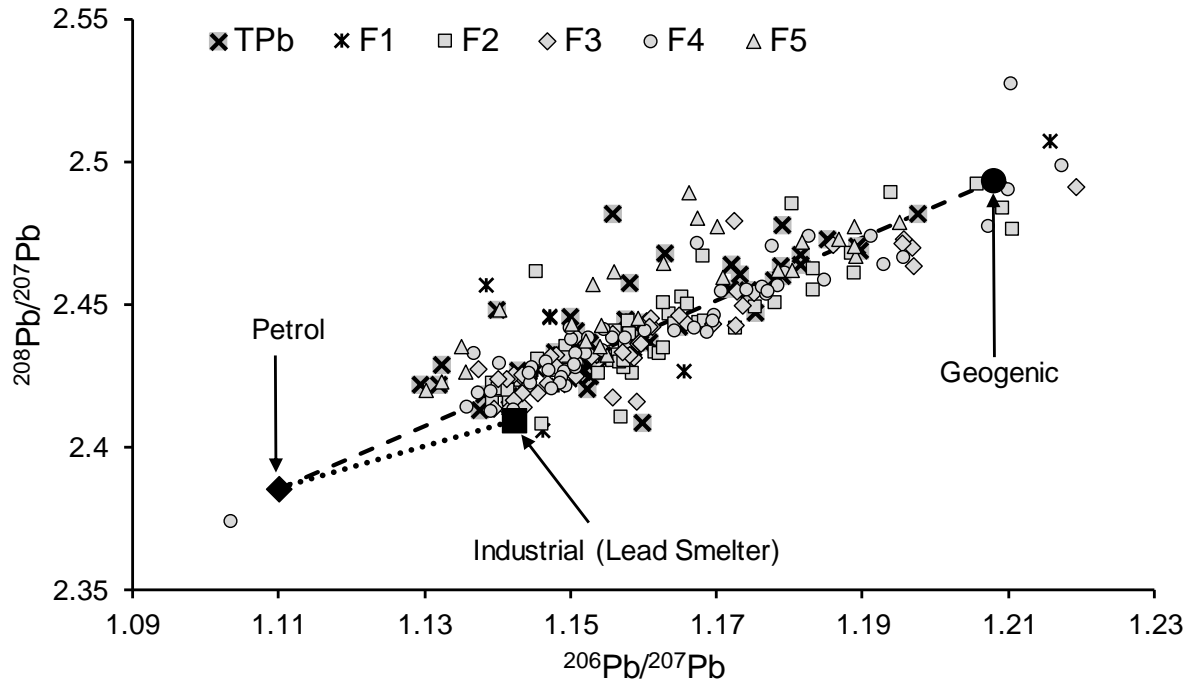
544

545



572 **Figure 5.** Proportion (%) of petrol-Pb (white boxes), industrial-Pb (light grey boxes) and geogenic-Pb (dark
573 grey boxes) in the total soil Pb (TPb) and the non-residual fractions F2, F3 and F4 in all sampling locations
574 excluding the SH-I (lead smelter) samples. Industrial-Pb signature was modelled by Solver from Eq. 3 and
575 Eq. 4 with the hypothesis that all end-members isotopic signatures are locate at the periphery of the dataset.
576 Numbers inside the boxes represent the proportion (%) of each fraction to total Pb in the respective soil
577 phase. Error bars represent the standard deviation between soils from the same location or soil type.

578



579

580

581 **Figure 6.** Anthropogenic-Pb isotopic ratios ($^{206}\text{Pb}/^{207}\text{Pb}$ vs $^{208}\text{Pb}/^{207}\text{Pb}$) of the whole soil and all five SEP
 582 fractions, in all soil samples. Petrol-Pb (black diamond), industrial-Pb (black square) and geogenic-Pb
 583 (black circle) signatures are also shown as possible end members. F5 fraction signatures are shown for
 584 samples where F5-Pb is $\geq 40\%$ of total soil Pb (TPb). Dashed line in the mixing line between petrol-Pb and
 585 geogenic-Pb signatures while the dotted line is the mixing line between petrol-Pb and industrial-Pb (lead
 586 smelter).

587

588

589

590

591

592

593

594

595

596 **4. Conclusions**

597 The concentrations of total soil Pb (TPb) in most of the studied soils were generally low and ranged around
598 the background and crustal Pb levels of ~ 5 and 14 mg kg⁻¹, respectively. Substantially elevated TPb levels
599 were only found in two industrial locations around a closed lead smelter (SH-I; ~ 16201 mg kg⁻¹) and a
600 waste water treatment facility (CA-I; ~ 171 mg kg⁻¹), and in two urban locations around major motorways
601 within Cairo (CA-U; ~160 mg kg⁻¹) and Alexandria (AX-U; ~ 83 mg kg⁻¹).

602 The residual fraction (F5-Pb) was the largest single fraction (38 - 63%) in all the studied locations with the
603 exception of SH-I and CA-I sites which were dominated by the carbonate (F2-Pb; 44%) and organic (F4-
604 Pb; 61%) fractions, respectively. Exchangeable Pb (F1-Pb) was only detectable in two locations: SH-I (1%
605 TPb; ~ 162 mg kg⁻¹) and CA-U (0.3% TPb; ~1.6 mg kg⁻¹). Although this may suggest that the current risk
606 of releasing considerable amounts of available Pb is exclusive to SH-I site (lead smelter), Pb in the other 3
607 non-residual fractions, in all locations including SH-I, may become available with any change in the soil
608 Eh/pH conditions. For example, in location CA-I (waste water treatment), if the conditions become more
609 oxidizing e.g. due to the waste treatment operations, the large organic (F4-Pb) pool will be released in
610 available forms. Therefore, in the four locations with elevated TPb levels (SH-I, CA-I, CA-U and AX-U),
611 despite their low/undetectable exchangeable-Pb, careful consideration should be taken to avoid mobilizing
612 hazardous amounts of Pb to the surrounding environments.

613 The non-residual Pb isotopic signatures (F1 – F4; ²⁰⁶Pb/²⁰⁷Pb) were dependent on the Pb source and level
614 of contamination; however, they displayed very similar patterns between the non-residual fractions (F2 -
615 F4). Similarly, the relative contribution of petrol-Pb to the non-residual Pb pools varied considerably
616 between sampling locations and was apparently controlled by the concentration of TPb despite being
617 almost identical in all the non-residual fractions (F2 - F4). This suggests no apparent difference in chemical
618 affinity of any given anthropogenic-Pb source for specific non-residual fractions in soil. Any initial source-
619 dependent distribution within the active soil fractions, following application to the soil, has apparently
620 disappeared with time.

621 It was not possible to identify a *single* 'third Pb source' to explain the distribution of Pb isotope ratios. A
622 major source, the Pb smelter in Cairo-Shubra, appeared to fall on the periphery of the dataset and could

623 be a significant contributor to Pb contamination in the country. However, removal of an assumed
624 background geogenic source produced a dataset in which the majority of Pb isotope ratios fell beyond the
625 range covered by the petrol and smelter sources. The suggestion is therefore that the majority of
626 'contaminant Pb' in Egypt has an isotopic signature close to that of geogenic Pb.

627

628 **Acknowledgments**

629 Waleed Shetaya acknowledges a postdoctoral fellowship (at the University of Nottingham, UK) funded by
630 the Egyptian Government.

631

632 **Conflicts of Interest**

633 The authors declare no conflicts of interest.

634

635 **Appendix A. Supplementary data**

636

637

638

639

640

641

642

643

644 **References**

- 645 Atkinson, N. R., Bailey, E. H., Tye, A. M., Breward, N. & Young, S. D. 2011. Fractionation of lead in soil
646 by isotopic dilution and sequential extraction. *Environmental Chemistry*, 8, 493-500.
- 647 Bacon, J. R., Farmer, J. G., Dunn, S. M., Graham, M. C. & Vinogradoff, S. I. 2006. Sequential extraction
648 combined with isotope analysis as a tool for the investigation of lead mobilisation in soils: Application to
649 organic-rich soils in an upland catchment in scotland. *Environmental pollution*, 141, 469-481.
- 650 Blum, J. D. & Bergquist, B. A. 2007. Reporting of variations in the natural isotopic composition of mercury.
651 *Analytical and Bioanalytical Chemistry*, 388, 353-359.
- 652 Brookins, D. G. 2012. *Eh-ph diagrams for geochemistry*, Springer Science & Business Media.
- 653 Chenery S. R., Izquierdo M., Marzouk E., Klinck B., Palumbo-Roe B., Tye A. M. 2012. Soil-plant
654 interactions and the uptake of Pb at abandoned mining sites in the Rookhope catchment of the N.
655 Pennines, UK—a Pb isotope study. *Science of the Total Environment*, 433, 547–560.
656
- 657 Cheng, H. & Hu, Y. 2010. Lead (pb) isotopic fingerprinting and its applications in lead pollution studies in
658 china: A review. *Environmental Pollution*, 158, 1134-1146.
- 659 Clevenger, T. E., Saiwan, C. & Koirtzohann, S. 1991. Lead speciation of particles on air filters collected in
660 the vicinity of a lead smelter. *Environmental science & technology*, 25, 1128-1133.
- 661 Cotter-Howells, J. & Thornton, I. 1991. Sources and pathways of environmental lead to children in a
662 derbyshire mining village. *Environmental Geochemistry and Health*, 13, 127-135.
- 663 Degryse, F., Smolders, E. & Parker, D. 2009. Partitioning of metals (cd, co, cu, ni, pb, zn) in soils:
664 Concepts, methodologies, prediction and applications—a review. *European Journal of Soil Science*, 60,
665 590-612.
- 666 Drummond, L. & Maher, W. 1995. Determination of phosphorus in aqueous-solution via formation of the
667 phosphoantimonylmolybdenum blue complex - reexamination of optimum conditions for the analysis of
668 phosphate. *Analytica Chimica Acta*, 302, 69-74.
- 669 Emsley, J. 2011. *Nature's building blocks: An az guide to the elements*, Oxford University Press.
- 670 Foster, R. L. & Lott, P. F. 1980. X-ray diffractometry examination of air filters for compounds emitted by
671 lead smelting operations. *Environmental Science & Technology*, 14, 1240-1244.
- 672 Harrison, R. M., Laxen, D. P. & Wilson, S. J. 1981. Chemical associations of lead, cadmium, copper, and
673 zinc in street dusts and roadside soils. *Environmental Science & Technology*, 15, 1378-1383.
- 674 Hassan, S. K., El-Abssawy, A. A., Abdel-Maksoud, A. S., Abdou, M. H. & Khoder, M. I. 2013. Seasonal
675 behaviours and weekdays/weekends differences in elemental composition of atmospheric aerosols in
676 cairo, egypt. *Aerosol and Air Quality Research*, 13, 1552-1562.
- 677 Hassanien, M. & Horvath, A. 1999. Lead risk assessment for children in hungary by predicting their blood
678 lead levels using us epa integrated exposure uptake biokinetic model. *Central European journal of public
679 health*, 7, 155-159.

- 680 Hassanien, M. A., Rieuwerts, J., Shakour, A. & Bittó, A. 2001. Seasonal and annual variations in air
681 concentrations of pb, cd and pahs in cairo, egypt. *International journal of environmental health research*,
682 11, 13-27.
- 683 Izquierdo, M., Tye, A. & Chenery, S. 2012. Sources, lability and solubility of pb in alluvial soils of the river
684 trent catchment, uk. *Science of the Total Environment*, 433, 110-122.
- 685 Komárek, M., Ettler, V., Chrastný, V. & Mihaljevič, M. 2008. Lead isotopes in environmental sciences: A
686 review. *Environment International*, 34, 562-577.
- 687 Kostka, J. E. & Luther, G. W. 1994. Partitioning and speciation of solid phase iron in saltmarsh sediments.
688 *Geochimica et Cosmochimica Acta*, 58, 1701-1710.
- 689 Labib, M. W., Safar, Z. & Khalil, M. H. 2003. Lead emission inventory in the greater cairo area during the
690 life time of caip. *AWMA paper*, 70137.
- 691 Lee, P.-K. & Yu, S. 2016. Lead isotopes combined with a sequential extraction procedure for source
692 apportionment in the dry deposition of asian dust and non-asian dust. *Environmental Pollution*, 210, 65-
693 75.
- 694 Li, X. & Thornton, I. 2001. Chemical partitioning of trace and major elements in soils contaminated by
695 mining and smelting activities. *Applied geochemistry*, 16, 1693-1706.
- 696 Luo, X.-S., Xue, Y., Wang, Y.-L., Cang, L., Xu, B. & Ding, J. 2015. Source identification and
697 apportionment of heavy metals in urban soil profiles. *Chemosphere*, 127, 152-157.
- 698 Mao, L. C., Bailey, E. H., Chester, J., Dean, J., Ander, E. L., Chenery, S. R. & Young, S. D. 2014. Lability
699 of pb in soil: Effects of soil properties and contaminant source. *Environmental Chemistry*, 11, 690-701.
- 700 Marzouk, E. R., Chenery, S. R. & Young, S. D. 2013a. Measuring reactive metal in soil: A comparison of
701 multi-element isotopic dilution and chemical extraction. *European Journal of Soil Science*, 64, 526-536.
- 702 Marzouk, E. R., Chenery, S. R. & Young, S. D. 2013b. Predicting the solubility and lability of zn, cd, and
703 pb in soils from a minespoil-contaminated catchment by stable isotopic exchange. *Geochimica Et*
704 *Cosmochimica Acta*, 123, 1-16.
- 705 McBride, M. 1994. Environmental soil chemistry. Oxford University Press, New York.
- 706 Meers, E., Du Laing, G., Unamuno, V., Ruttens, A., Vangronsveld, J., Tack, F. M. & Verloo, M. G. 2007.
707 Comparison of cadmium extractability from soils by commonly used single extraction protocols.
708 *Geoderma*, 141, 247-259.
- 709 Mohamed, E. F., El-Hashemy, M. A., Abdel-Latif, N. M. & Shetaya, W. H. 2015. Production of sugarcane
710 bagasse-based activated carbon for formaldehyde gas removal from potted plants exposure
711 chamber. *Journal of the Air & Waste Management Association*, 65, 1413-1420.
712
- 713 Monna, F., Lancelot, J., Croudace, I. W., Cundy, A. B. & Lewis, J. T. 1997. Pb isotopic composition of
714 airborne particulate material from france and the southern united kingdom: Implications for pb pollution
715 sources in urban areas. *Environmental Science & Technology*, 31, 2277-2286.
- 716 Murphy, S. 1992. Smelting residues from boles and simple smeltermills. *Boles and smeltermills*, 43-47.
- 717 Nasralla, M. & Ali, E. 1984. Lead, cadmium and zinc around traffic roads. *Egyptian J. Occupat. Med*, 8,
718 197-210.

- 719 Needleman, H. L. & Bellinger, D. 1991. The health effects of low level exposure to lead. *Annual Review of*
720 *Public Health*, 12, 111-140.
- 721 Olsen, S. R., Cole, C. V., Watanabe, F. S. & Dean, L. A. 1954. Estimation of available phosphorus in soils
722 by extraction with sodium bicarbonate. *U.S. Dep. of Agric. Circ*, 939.
- 723 Rizk, H. F. & Khoder, M. I. 2001. Decreased lead concentration in cairo atmosphere due to use of
724 unleaded gasoline. *Central European Journal of Occupational and Environmental Medicine Hungary*.
- 725 Roebbert, Y., Rabe, K., Lazarov, M., Schuth, S., Schippers, A., Dold, B. & Weyer, S. 2018. Fractionation
726 of fe and cu isotopes in acid mine tailings: Modification and application of a sequential extraction
727 method. *Chemical Geology*, 493, 67-79.
- 728 Safar, Z., Labib, M. W., Lotfi, W. & Khalil, M. H. 2014. Characterization of contamination around the
729 largest lead smelter in egypt carried out through a cooperation program between USA and egypt. *Field*
730 *Actions Science Reports. The journal of field actions*, 7.
- 731 Safar, Z. S. & Labib, M. W. 2010. Assessment of particulate matter and lead levels in the greater cairo
732 area for the period 1998–2007. *Journal of advanced research*, 1, 53-63.
- 733 Sastre, J., Rauret, G. & Vidal, M. 2006. Effect of the cationic composition of sorption solution on the
734 quantification of sorption–desorption parameters of heavy metals in soils. *Environmental pollution*, 140,
735 322-339.
- 736 Shaheen, S. M. 2009. Sorption and lability of cadmium and lead in different soils from egypt and greece.
737 *Geoderma*, 153, 61-68.
- 738 Shakour, A. & El-Taieb, N. 1994. Effect of atmospheric lead exposure on urban children. *Egyptian J*
739 *Occup Med*, 18, 37-47.
- 740 Shetaya, W. H., Marzouk, E. R., Mohamed, E. F., Elkassas, M., Bailey, E. H. & Young, S. D. 2018. Lead
741 in egyptian soils: Origin, reactivity and bioavailability measured by stable isotope dilution. *Science of The*
742 *Total Environment*, 618, 460-468.
- 743 Shetaya, W. H., Osterwalder, S., Bigalke, M., Mestrot, A., Huang, J.-H. & Alewell, C. 2017. An isotopic
744 dilution approach for quantifying mercury lability in soils. *Environmental Science & Technology Letters*, 4,
745 556-561.
- 746 Sparks, D. L. 2003. *Environmental soil chemistry*, Academic Press, An imprint of Elsevier Science,
747 California, USA.
- 748 Tack, F. & Verloo, M. G. 1995. Chemical speciation and fractionation in soil and sediment heavy metal
749 analysis: A review. *International Journal of Environmental Analytical Chemistry*, 59, 225-238.
- 750 Tessier, A., Campbell, P. G. C. & Bisson, M. 1979. Sequential extraction procedure for the speciation of
751 particulate trace-metals. *Analytical Chemistry*, 51, 844-851.
- 752 Teutsch, N., Erel, Y., Halicz, L. & Banin, A. 2001. Distribution of natural and anthropogenic lead in
753 mediterranean soils. *Geochimica et Cosmochimica Acta*, 65, 2853-2864.
- 754 Tipping, E., Thompson, D., Ohnstad, M. & Hetherington, N. 1986. Effects of ph on the release of metals
755 from naturally-occurring oxides of mn and fe. *Environmental Technology*, 7, 109-114.
- 756 Tongtavee, N., Shiowatana, J., McLaren, R. G. & Gray, C. W. 2005. Assessment of lead availability in
757 contaminated soil using isotope dilution techniques. *Science of the Total Environment*, 348, 244-256.

- 758 Veysseyre, A. M., Bollhöfer, A. F., Rosman, K. J., Ferrari, C. P. & Boutron, C. F. 2001. Tracing the origin
759 of pollution in french alpine snow and aerosols using lead isotopic ratios. *Environmental science &*
760 *technology*, 35, 4463-4469.
- 761 Who 2010. Exposure to lead: A major public health concern. Preventing disease through healthy
762 environments. Geneva, World Health Organization (<http://www.who.int/ipcs/features/lead..pdf>) 6.
- 763 Young, S. D., Tye, A., Carstensen, A., Resende, L. & Crout, N. 2000. Methods for determining labile
764 cadmium and zinc in soil. *European Journal of Soil Science*, 51, 129-136.